Computation Offloading and Resource Allocation in LEO Satellite-Terrestrial Integrated Networks With System State Delay

Bo Xie, Haixia Cui, *Senior Member, IEEE*, Ivan Wang-Hei Ho, *Senior Member, IEEE*, Yejun He, *Senior Member, IEEE*, and Moshen Guizani, *Fellow, IEEE*

***Abstract*—Computing offloading optimization for energy saving is becoming increasingly important in low-Earth orbit (LEO) satellite-terrestrial integrated networks (STINs) since battery techniques has not kept up with the demand of ground terminal devices. In this paper, we design a delay-based deep reinforcement learning (DRL) framework specifically for computation offloading decisions, which can effectively reduce the energy consumption. Additionally, we develop a multi-level feedback queue for computing allocation (RAMLFQ), which can effectively enhance the CPU's efficiency in task scheduling. We initially formulate the computation offloading problem with the system delay as Delay Markov Decision Processes (DMDPs), and then transform them into the equivalent standard Markov Decision Processes (MDPs). To solve the optimization problem effectively, we employ a double deep Q-network (DDQN) method, enhancing it with an augmented state space to better handle the unique challenges posed by system delays. Simulation results demonstrate that the proposed learning-based computing offloading algorithm achieves high levels of performance efficiency and attains a lower total cost compared to other existing offloading methods.**

***Index Terms*—Computing offloading, satellite-terrestrial integrated networks, system state delays in learning, deep reinforcement learning.**

I. Introduction

Advances in satellite constellations are revolutionizing internet access, which extends communication services to every corner of the Earth, including underdeveloped areas with limited infrastructure, like remote regions and oceans. These developments have led to the construction of satellite-terrestrial integrated networks which can connect numerous edge devices. A groundbreaking aspect of satellite-terrestrial integrated networks (STINs) is providing computational resources through satellites, a paradigm shift that takes the low-Earth orbit satellite (LEOS) as new edge servers [1]. This transformation not only improves communication capabilities but also opens up new possibilities in global data processing and management.

However, integrating advanced artificial intelligence (AI) applications at the edge, linking end users with LEO satellites and the cloud, poses significant new challenges. The inherently distributed and dynamic nature of the edge environment complicates such deployments, and the high computational demands of AI applications limit their use on resource-constrained edge devices. To overcome these obstacles, some efforts have been directed towards offloading computationally intensive tasks to cloud servers, edge servers, and LEO servers, utilizing their processing power to manage the computational load of sophisticated AI applications [2]–[5].

Deep reinforcement learning (DRL) has recently been employed to tackle the computation offloading challenges in STINs [6]–[8], where the DRL agent interacts with the environment through a trial-and-error process, making decisions based on the observable system states and receiving feedback in the form of rewards and new states. However, practical challenges arise due to the inherent network latency, computational bottlenecks, and the time required for task execution, all of which introduce significant delays in the observable states and decision execution [9], [10]. These delays force the DRL agent to operate with outdated information, requiring it to make effective offloading decisions based on past states and actions [11]. The challenge lies in how to utilize this outdated information to guide the agent in making optimal decisions despite the inherent uncertainties. Although DRL is increasingly applied in this context, existing studies often overlook the impact of these delays, assuming that system states and feedback can be obtained instantaneously. This gap underscores the need for more realistic models that account for the inevitable delays in DRL-based offloading decisions.

This paper introduces a flexible joint communication and computation framework for STINs, designed to provide robust computing services to remote users through edge/cloud/satellite integration. We propose an efficient computing offloading approach that learns an optimal offloading policy on-the-fly, aiming to minimize the energy consumption. This takes into account the multidimensional network dynamics, resource constraints, and system state/action delays. We first formulate the computation offloading problem with system state delays as stochastic delay MDPs (SDMDPs), demon-

Manuscript received xx. 2024. This work was supported in part by National Key Research and Development Program of China under Grant 2023YFE0107900, in part by the GuangDong Basic and Applied Basic Research Foundation under Grant 2024A1515012052, in part by the National Natural Science Foundation of China under grants 61871433, 61828103, 61201255, and 62071306, and in part by the Research Platform of South China Normal University.

Bo Xie and Haixia Cui are with the School of Electronics and Information Engineering, South China Normal University, Foshan 528225, China (e-mail: bo.xie@m.scnu.edu.cn; cuihaixia@m.scnu.edu.cn).

Wang-Hei Ho is with the Department of Electrical and Electronic Engineering, The Hong Kong Polytechnic University, Hong Kong, China (e-mail: ivanwh.ho@polyu.edu.hk).

Yejun He is with the College of Electronics and Information Engineering, Shenzhen University, Shenzhen 518060, China (e-mail: heyejun@126.com).

Mohsen Guizani is with the Mohamed Bin Zayed University of Artificial Intelligence (MBZUAI), UAE (email: mguizani@ieee.org).

strating how to reduce these to MDPs without delays. We then propose a model-free, delay-based reinforcement learning approach to seek an optimal offloading mode. Finally, we deploy a computing allocation algorithm on each edge server, based on a multi-level feedback queue. To our knowledge, this work is the first to study the computation offloading problem in STINs with system state delays. It validates the feasibility of STINs in supporting computation-intensive applications for remote users and offers useful guidelines for remote computing offloading.

The main contributions of the paper can be summarized as follows.

- We introduce an innovative framework designed to enhance computing services in STINs. This framework that integrates edge, cloud, and satellite technologies is tailored to address the unique challenges of STINs, such as resource constraints and system state delays. This approach is particularly beneficial for remote users, who typically face limited access to robust computing services.
- We formulate the computation offloading problem in STINs with system state delays as SDMDPs. We demonstrate how these processes can be effectively transformed into simpler MDPs without delays. Building on this foundation, we propose a model-free, delay-based reinforcement learning approach to seek an efficient computing offloading strategy aimed at minimizing the impact of energy consumption. Additionally, we have developed a multi-level feedback queue-based computing allocation algorithm for each edge server, addressing a novel area in the computation offloading domain and offering practical solutions for computation-intensive applications in remote areas.
- The efficacy of our proposed approaches is rigorously evaluated through extensive simulations. This evaluation provides valuable insights into the practical applicability and efficiency of our methods in real-world scenarios.

The remainder of the paper is organized as follows. In Section II, we present the related work. Section III describes the system model. In Section IV, the joint edge computing allocation and computation offloading problem is formulated and solved. Section V introduces the SDMDPs. Section VI formulates the DRL-based solution. Section VII evaluates the proposed approaches, and Section VIII concludes the paper.

II. Related Work

In the realm of satellite-terrestrial integrated networks, computation offloading methods play a pivotal role. Broadly, these methods fall into two categories: mathematical-based and intelligence-based approaches [12]–[15]. Central to this discussion is the interplay between computation offloading and resource allocation strategies, a key area of focus in network optimization.

A. Mathematical Offloading Method

Satellite-terrestrial edge computing is conceptualized as a three-tier architecture encompassing space, air, and ground, with the ground tier also extending to marine or aquatic environments. Specifically, the space tier primarily includes low-earth orbit and geosynchronous (GEO) satellites. The air tier encompasses various aerial vehicles like aircraft and drones, while the ground tier comprises communication infrastructure, Internet of Things (IoT) devices, and vehicles. In marine settings, vessels are commonly used, and underwater sensors or servers can be deployed in aquatic environments. Researchers primarily aim to optimize computation offloading and resource allocation performance within this intricate, integrated network [16]–[18]. This optimization is based on network characteristics, with a focus on minimizing system energy consumption and reducing the computing latency.

Researchers aim to optimize this complex network, focusing on minimizing system energy consumption and reducing computing latency, a task that involves balancing the unique characteristics of each network tier. For instance, the majority of communication terminals in the terrestrial network offload tasks to satellites using Ka-band wireless backhaul connections, with the satellites then returning processed results via either Ka-band or C-band connections [19], [20]. The challenge lies in managing the computational workloads, especially given the dynamic nature of these networks. A notable solution proposed involves using the Lyapunov framework for optimizing the objective function [2], [19], [21]–[23].

Incorporating high-altitude aircraft into the network introduces new complexities due to their variable speeds and trajectories, which constantly change network topologies. Addressing these challenges, recent studies [3], [24]–[27] have focused on optimizing the trajectory of unmanned aerial vehicles (UAVs) and using iterative algorithms for more efficient offloading and resource allocation.

Furthermore, cloud data centers have emerged as significant players in this network, acting as communication relays for remote users [4]. The computation offloading decision in this context becomes a binary problem: to offload tasks either to satellites or cloud data centers. This discrete and non-convex problem has been transformed into a linear programming problem for more effective resolution [4].

These studies provide a foundation for our approach in this paper, offering insights into managing dynamic network environments and leveraging the power of neural networks for better generalization in addressing these challenges.

B. Intelligence Offloading Method

Traditionally, satellite-terrestrial integrated networks have relied on objective functions resolved through optimization algorithms. However, the advent of deep learning, particularly supervised methods, has revolutionized this approach [28], [29]. By training neural networks with data derived from traditional methods, we can now obtain offloading decisions and resource allocation values instantaneously, a significant leap from the slower resolution of conventional techniques.

DRL has emerged as a powerful tool in this landscape. Cui et al. [30] implemented a Double Deep Q-Network (DDQN) for computation offloading alongside traditional algorithms for resource allocation, addressing the challenges posed by the dynamic nature of satellite coverage areas and user link

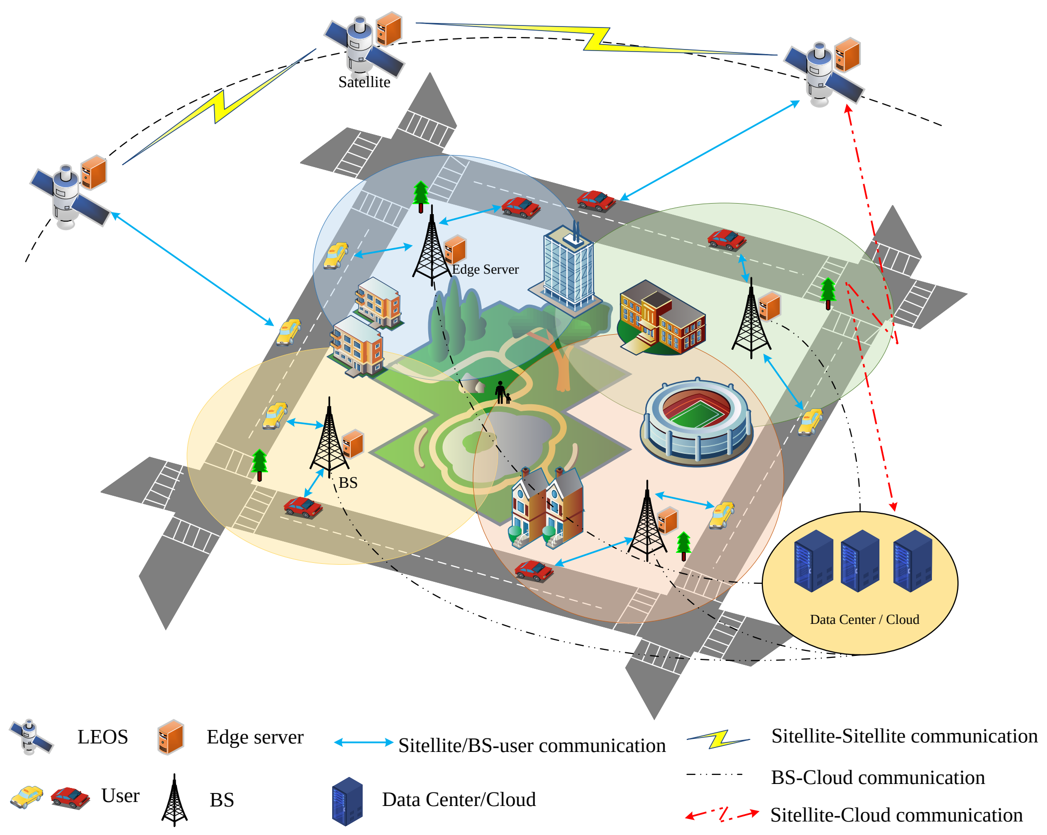

Fig. 1. LEO-STIN scenario.

quality. Similarly, Zhang et al. [31] and other researchers [32], [33] have explored various DRL-based methods to manage the complexities of computation offloading and resource allocation in these networks.

Tang et al. [5] emphasized a long-term performance strategy, combining DRL for computation offloading with Lyapunov optimization for resource allocation. This approach, also reflected in other studies [6], involves predicting network resource variations and developing online algorithms for more accurate forecasting.

In applying digital twin technology to satellite-terrestrial integrated networks, Ji et al. [7] identified a delay in updating network status information but posited that DRL could address this issue [8]. However, their focus was limited to the algorithmic perspective, omitting broader considerations of systemic update delays. This phenomenon of state delay was similarly observed in studies [9], [10].

Finally, our research builds upon these insights, particularly focusing on the challenges posed by state delays within the system. We use DRL for computation offloading, complemented by traditional methodologies for computing resource allocation, to navigate the complexities of satellite-terrestrial integrated networks effectively.

III. System Model

Consider a LEO-STIN scenario consisting of M low Earth orbit satellites $\mathcal{M} = \{1, 2, \cdots, m, \cdots, M\}$, N terrestrial base stations (BSs) $\mathcal{N} = \{1, 2, \cdots, n, \cdots, N\}$, K mobile users $\mathcal{K} = \{1, 2, \cdots, k, \cdots, K\}$, and a cloud data center (CDC), as illustrated in Fig. 1. Each mobile user handles k diverse tasks which vary in computational requirements and can be offloaded to BSs, CDC, LEO satellites, or locally. The network operates in fixed time slots $t \in \{0, 1, 2, \cdots, \tau\}$ where τ represents the finite time horizon. The task from user k at time t is represented as $\Lambda_k^t = \{s_k^t, r_k^t, c_k^t, z_{k,max}^t\}$. Here, s_k^t is the data size, r_k^t is the feedback data size, c_k^t is the necessary clock cycles for completion, and $z_{k,max}^t$ is the maximum latency. To simplify, we assume that $z_{k,max}^t$ is sufficiently large to prevent task failure due to timeouts.

The users can process the tasks locally or offload them to the satellites, base stations, or cloud data center. The transmission rate between satellites is assumed to be very fast with negligible delay [38], [39]. Consequently, the tasks need only to be offloaded to the nearest satellite based on its current position. The offloading decision for user k at time t is represented as $\mathcal{X}(t,k) \in \{0, \mathcal{N}, N+1, N+2\}$, *i.e.*,

$$\mathcal{X}(t,k) = \begin{cases} 0, & \text{processed locally}, \\ \mathcal{N}, & \text{offloaded to BSs}, \\ N+1, & \text{offloaded to LEOS}, \\ N+2, & \text{offloaded to CDC}. \end{cases} \tag{1}$$

Here, $N+1$ represents offloading the task to a satellite. Since we ignore the delay between satellites, we choose the most suitable satellite node from the LEOS set $\mathcal{M}$ based on the location of user k [4].

The offloading tasks can occur via the wireless backhaul links. For the links between BSs and LEO satellites, the C-band and Ka-band are utilized, respectively. Additionally, the users can offload the tasks to the CDC through either LEO satellites or BSs. The link between BSs and CDC is facilitated by the ethernet, while the link between LEO satellites and CDC uses the wireless backhaul links on Ka-band.

A. Communication Model

1) Terrestrial Communications: The achievable capacity by user k with service of base station n over C-band can be expressed by

$$R_{n,k} = \psi_k B_C \log_2 \left(1 + \frac{p_{n,k}|h_{n,k}^C|^2}{\delta^2}\right), \tag{2}$$

where B_C represents the total bandwidth in the C-band. The factor $\sum_{k=1}^{K} \psi_k = 1$ indicates that ψ_k allocates bandwidth to user k at BS n. The transmit power and noise variance are represented by $p_{n,k}$ and δ^2, respectively, while $h_{n,k}^C$ indicates the channel gain between user k and BS n.

The channel gain, $h_{n,k}^C$, is predominantly affected by the Line-of-Sight (LoS) path is written by

$$h_{n,k}^C = \xi d_{k,n}^{-\alpha}, \tag{3}$$

where $d_{k,n}^{-\alpha}$ is used for calculating the path loss between user k and BS n. ξ is the unity channel gain at a reference distance of 1 meter. The path loss exponent is denoted by α.

2) LEOS Communications: The capacity achievable by user k when served by LEO m over the Ka-band is given by:

$$R_{m,k} = \hat{\psi}_k B_{Ka} \log_2 \left(1 + \frac{p_{m,k}|h_{m,k}^{Ka}|^2}{\hat{\delta}^2}\right), \tag{4}$$

where B_{Ka} denotes the total bandwidth in the Ka-band. The term $\sum_{k=1}^{K} \hat{\psi}_k = 1$ indicates that $\hat{\psi}_k$ is a bandwidth allocation factor for user k at LEO m. The transmit power and noise variance are represented by $p_{m,k}$ and $\hat{\delta}^2$. The channel gain between user k and LEO m is $h_{m,k}^{Ka}$, defined as:

$$h_{m,k}^{Ka} = \gamma \hat{d}_{k,m}^{-\beta}, \tag{5}$$

which takes the path loss between user k and LEO m as a function of their distance. The term γ corresponds to log-normal distributed shadow fading, and β is the path loss exponent.

The model in (4) also need calculate the achievable communication capacity between satellites and cloud data centers as well as between satellites and base stations.

B. Computing Model

This system includes various computing models: local computing, base station server-aided computing, cloud data center server-aided computing, and low earth orbit satellite edge-aided computing. We adopt a partial offloading approach, where tasks are either processed locally or offloaded to the BS server, cloud data center, or LEOS edge.

1) Local Computing: For a task Λ_k^t partially processed locally at time t, the computing time, $D_{k,loc}^t$, is given by:

$$D_{k,loc}^t = \frac{c_k^t}{f_k}, \tag{6}$$

where f_k represents the computation capability of user k in CPU cycles per second.

2) BS Server Computing: BS server computing includes transmission latency and BS server computation time. Let $f_{n,max}$ and $f_{n,k}$ denote the maximum CPU cycles at BS n server for user k. Assuming equal uplink and downlink rates [44], the total latency, $D_{k,n}^t$, is:

$$D_{k,n}^t = \frac{s_k^t + r_k^t}{R_{n,k}} + \frac{c_k^t}{f_{n,k}}. \tag{7}$$

3) Cloud Data Center Computing: This model includes transmission and execution time at the cloud data center. Assuming infinite resources, the maximum CPU cycles f_{max}^{cloud} are utilized. Tasks can be offloaded through the base station or directly via satellite. The total latency, $D_{k,cloud}^t$, is:

$$\begin{aligned} D_{k,cloud}^t = {} & \delta \left(\frac{s_k^t + r_k^t}{R_{m,k}} + \frac{s_k^t + r_k^t}{R_{m,cloud}} + \frac{c_k^t}{f_{max}^{cloud}}\right) \\ & + (1-\delta)\left(\frac{s_k^t + r_k^t}{R_{n,k}} + \frac{s_k^t + r_k^t}{R_{n,cloud}} + \frac{c_k^t}{f_{max}^{cloud}}\right), \end{aligned} \tag{8}$$

where $\delta \in \{0, 1\}$ indicates the offloading route: 0 for the base station, 1 for satellite.

4) LEOS Edge Computing: LEOS edge computing consists of transmission time and LEOS server execution time. Let $f_{m,max}$ and $f_{m,k}$ be the maximum CPU cycles at the LEOS server for user k. The total latency, $D_{k,m}^t$, is:

$$D_{k,m}^t = \frac{s_k^t + r_k^t}{R_{m,k}} + \frac{c_k^t}{f_{m,k}}. \tag{9}$$

LEO satellites can collaboratively process tasks via inter-satellite links (ISLs), especially under high offloading demands, with minimal transmission delays [38], [45].

The offloading latency for user k at time t is:

$$D_k^t = \begin{cases} D_{k,loc}^t, & \text{if } \mathcal{X}(t,k) = 0 \\ D_{k,n}^t, & \text{if } \mathcal{X}(t,k) \in \mathcal{N} \\ D_{k,m}^t, & \text{if } \mathcal{X}(t,k) = N+1 \\ D_{k,cloud}^t, & \text{if } \mathcal{X}(t,k) = N+2. \end{cases} \tag{10}$$

The total computing time can be calculated as

$$D = \sum_{t=0}^{\tau} \sum_{k=1}^{K} D_k^t \tag{11}$$

where K represents the number of users.

C. Energy Model

This section details the energy consumption in various computing scenarios, including local processing, BS processing, cloud data center processing, and LEOS edge processing.

1) Executing Energy: The power consumption for local processing, denoted as p_l, is assumed to be the same for all users. The energy required for local processing is:

$$E_{k,loc}^{t,exe} = p_l \frac{c_k^t}{f_k}. \tag{12}$$

In LEOS edge processing, with a constant energy dissipation rate p_{leo}, the energy requirement is:

$$E_{k,leo}^{t,exe} = p_{leo} \frac{c_k^t}{f_{m,k}}. \tag{13}$$

For cloud data center processing, the energy dissipation rate is p_{cloud}, leading to:

$$E_{k,cloud}^{t,exe} = p_{cloud} \frac{c_k^t}{f_{max}^{cloud}}. \tag{14}$$

In BS processing, with an energy dissipation rate p_{bs}, the energy requirement is:

$$E_{k,bs}^{t,exe} = p_{bs} \frac{c_k^t}{f_{n,k}}. \tag{15}$$

The overall executing energy dissipation is determined by the computing scenario:

$$E_k^{t,exe} = \begin{cases} E_{k,loc}^{t,exe}, & \text{if } \mathcal{X}(t,k) = 0 \\ E_{k,bs}^{t,exe}, & \text{if } \mathcal{X}(t,k) \in \mathcal{N} \\ E_{k,leo}^{t,exe}, & \text{if } \mathcal{X}(t,k) = N+1 \\ E_{k,cloud}^{t,exe}, & \text{if } \mathcal{X}(t,k) = N+2. \end{cases} \tag{16}$$

2) Transmitting Energy: The energy dissipation during transmission depends on the destination of the data. For transmission to the LEOS edge:

$$E_{k,m}^{t,trans} = p_k \frac{s_k^t + r_k^t}{R_{m,k}}. \tag{17}$$

For transmission to the cloud data center:

$$\begin{aligned} E_{k,cloud}^{t,trans} = p_k^{cloud} \cdot \Bigg[&\delta \left(\frac{s_k^t + r_k^t}{R_{m,k}} + \frac{s_k^t + r_k^t}{R_{m,cloud}} \right) \\ &+ (1-\delta) \left(\frac{s_k^t + r_k^t}{R_{n,k}} + \frac{s_k^t + r_k^t}{R_{n,cloud}} \right) \Bigg], \end{aligned} \tag{18}$$

where $\delta \in \{0,1\}$ indicates the offloading route: 0 for the base station, 1 for satellite.

For transmission to the BS:

$$E_{k,bs}^{t,trans} = p_k^{bs} \frac{s_k^t + r_k^t}{R_{n,k}}. \tag{19}$$

The total energy dissipation for transmission is:

$$E_k^{t,trans} = \begin{cases} E_{k,loc}^{t,trans}, & \text{if } \mathcal{X}(t,k) = 0 \\ E_{k,bs}^{t,trans}, & \text{if } \mathcal{X}(t,k) \in \mathcal{N} \\ E_{k,leo}^{t,trans}, & \text{if } \mathcal{X}(t,k) = N+1 \\ E_{k,cloud}^{t,trans}, & \text{if } \mathcal{X}(t,k) = N+2. \end{cases} \tag{20}$$

Finally, the total energy consumption is calculated as [32]:

$$E = \varphi \cdot \sum_{t=0}^{\tau} \sum_{k=1}^{K} E_k^{t,exe} + \sum_{t=0}^{\tau} \sum_{k=1}^{K} E_k^{t,trans}, \tag{21}$$

where K represents the number of users, $\varphi \in (0,1)$ is a factor used primarily to balance the execution energy consumption and the transmission energy consumption.

IV. PROBLEM FORMULATION

A. Objective Function

We aim at jointly optimizing the computation offloading and resource allocation to minimize the energy consumption under the user latency constraints. It involves the optimization of offloading decision vector $\mathcal{X}(t,k)$, BS server computing resource allocation matrix $F^{\mathcal{N}}$, LEOS edge computing resource allocation matrix $F^{\mathcal{M}}$, and bandwidth resource allocation matrix P. Therefore, the optimization problem is formulated by

$$\mathcal{P}0: \min_{\{\mathcal{X}, F^{\mathcal{N}}, F^{\mathcal{M}}\}} \quad E, \tag{22a}$$

$$\text{s.t.} \quad E^{trans} > 0, E^{exe} > 0, \tag{22b}$$

$$f_{n,k} > 0, f_{m,k} > 0, \forall n \in \mathcal{N}, \forall m \in \mathcal{M}, \forall k \in \mathcal{K}, \tag{22c}$$

$$\psi_k \in (0,1), \hat{\psi}_k \in (0,1), \forall k \in \mathcal{K}, \tag{22d}$$

$$\sum_{k \in \mathcal{K}_{bs}} \psi_k = 1, \tag{22e}$$

$$\sum_{k \in \mathcal{K}_{leo}} \hat{\psi}_k = 1, \tag{22f}$$

$$D \le \sum_{t=0}^{\tau} \sum_{k \in \mathcal{K}} z_{k,max}^t, \tag{22g}$$

$$\sum_{k \in \mathcal{K}_{bs}} f_{n,k} \le f_{n,max}, \forall n \in \mathcal{N}, \tag{22h}$$

$$\sum_{k \in \mathcal{K}_{leo}} f_{m,k} \le f_{m,max}, \forall m \in \mathcal{M}, \tag{22i}$$

$$\mathcal{X}(t,k) \in \{0, \mathcal{N}, N+1, N+2\}, \forall k \in \mathcal{K}, \tag{22j}$$

where $\mathcal{K}_{bs}$ and $\mathcal{K}_{leo}$ represent the users served by the BS and LEO, respectively.

The constraints in $\mathcal{P}0$ are detailed as follows: (22b) guarantees that the computation tasks are executed while (22c) ensures that each task is allocated appropriate resources. (22d), (22e), and (22f) represent that the allocated bandwidth resources will not exceed the upper limit of BS or LEO. (22g) indicates that offloading tasks is effective. (22h) and (22i) respectively indicate that the computation resources allocated to the tasks by the base station and satellite will not exceed their total computation resources. (22j) means that the tasks will be executed locally or offloaded to base stations or satellites.

$\mathcal{P}0$ aims to obtain the optimal values of $\mathcal{X}, F^{\mathcal{N}}$, and $F^{\mathcal{M}}$ for users. Since the offloading decision variable $\mathcal{X}$ is discrete in contrast to $F^{\mathcal{N}}$ and $F^{\mathcal{M}}$ which vary continuously and dynamically, $\mathcal{P}0$ is a mixed integer nonlinear programming (MINLP) problem and it falls into NP-hard. Given the dynamic and time-sensitive nature of networks, it is difficulty to achieve an optimal solution through traditional computation methods and the computational time is non-polynomial. To address this issue, we will propose a solution method based on DRL as follows.

B. Offloading Policy Model

We define the offloading policy model as SDMDP represented by $\langle \mathcal{S}, \mathcal{A}, P_A, R, O, AC, C, \gamma \rangle$ in which the random variables represent the finite state space, available actions, transition probabilities, rewards, delays in observation, action, cost, and discount factor, respectively. In Section V, we will convert it into a standard MDP to solve the offloading challenge in $\mathcal{P}0$ based on DRL.

C. Optimization of Computing Resource Allocation

Due to the dynamic computing environments and heterogeneous task requirements, the traditional computing resource optimization methods are very challenging because they cannot rapidly respond to the multi-dimensional characteristic of $\mathcal{P}0$. Inspired by the work in [37], we propose a novel computing resource allocation algorithm, RAMLFQ, to optimize the computing resource allocation for task offloading in BS servers and LEOS edge computing. It can ensure good real-time performance while taking into account the computing resource requirements, priority, and resource limits of tasks. We dynamically adjust the CPU resource allocation strategy based on these factors. Formally, let $\Lambda^t = \{\Lambda_1^t, \Lambda_2^t, \cdots, \Lambda_K^t\}$ be the task served by the base station n with total computing resource $f_{n,max}$, in time slot t. Let c_k^t, p_k^t, $f_{n,k}^t$ be the required computing resource of the task Λ_k^t, the priority of the task Λ_k^t, and the allocated computing resource in time slot t, respectively. Note that the resource allocation strategy needs to satisfy (22h). Then, the basic resource allocation for each task can be defined as

$$f_{n,base} = \frac{f_{n,max}}{2|\Lambda^t|}, \tag{23}$$

where $|\Lambda^t|$ is the number of tasks.

Similarly, the remaining CPU resources are defined as

$$f_{n,extra} = f_{n,max} - |\Lambda^t| \cdot f_{n,base}. \tag{24}$$

Taking into account the priority of tasks and dynamic allocation of CPU resources required by each task, the dynamic resource allocation strategy for each task is defined as

$$f_{n,k}^t = f_{n,base} + \min\left(c_k^t - f_{n,base}, \frac{f_{n,extra} \times (w_1(p_k^t) + w_2(Q_k))}{\sum_{k=1}^K (w_1(p_k^t) + w_2(Q_k))}\right), \tag{25}$$

where w_1 and w_2 are the weights of task priority and priority queue, respectively.

We use a linear function as the weight parameter, *i.e.*,

$$w_1(p_k^t) = a \cdot p_k^t + b, \tag{26}$$

$$w_2(Q_k) = c \cdot k + d, \tag{27}$$

where $a, b, c, d \in \mathbb{R}$ are weight coefficients and $k \in \mathbb{Z}^+$ is the index of priority queue.

This algorithm includes a scheduling strategy that adopts a time-slice round-robin system. Here, we define the time-slice parameter according to (25). Except for the time-slice round-robin scheduling strategy, this algorithm also aims to ensure the real-time performance of tasks because it need be implemented in all base stations and satellites.

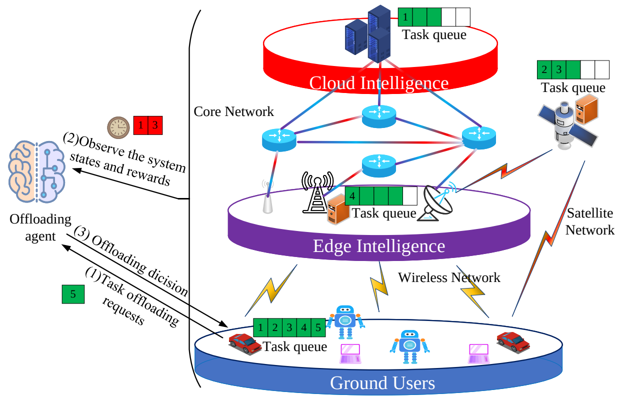

Fig. 2. The computation offloading process in a LEO-STIN scenario.

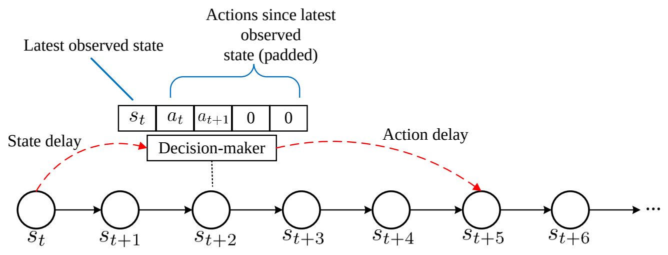
Latest observed state
Actions since latest observed state (padded)
s_t a_t a_{t+1} 0 0
State delay
Decision-maker
Action delay
s_t s_{t+1} s_{t+2} s_{t+3} s_{t+4} s_{t+5} s_{t+6} ...

Fig. 3. Graphical illustration of the problem of the LEO satellite-terrestrial integrated networks with system state delay.

V. Markov Decision Processes with Delays

We formulate the corresponding MDPs with delays for modeling the dynamic LEO STINs and the task offloading process is shown in Fig. 2. The user initially submits a task offloading request and then the agent selects the optimal action based on the currently observed system state to make the offloading decision which will be executed by the user. Crucially, the agent does not immediately receive updates on the state and corresponding rewards after the task is offloaded. It needs to wait for several moments as the system requires time to process and respond to the offloading action. Moreover, due to the heterogeneity of user devices, the processing speeds and completion timings of different tasks are different, causing the states and rewards received by the agent at a future moment be potentially influenced by other concurrent actions. Under these circumstances, the agent faces a complex and dynamically changing environment, woven together by multiple influencing factors. For example, as depicted in Fig. 2, the agent sequentially offloads Task 1 to a cloud data center, while Tasks 2 and 3 are offloaded to a satellite, and Task 4 to an edge server. Subsequently, when the agent receives a request to offload Task 5, due to network latency and the heterogeneity of devices, it can only observe the states and rewards of Tasks 1 and 3, as the execution of Tasks 2 and 4 has not yet completed, thus precluding the acquisition of their states and rewards. In this scenario, the observed state and reward information by the agent exhibits delays.

Intuitively, as shown Fig. 3, it is illustrated that when the agent makes a decision at time $t+2$, it can only observe the system state from time t, which is the most recent system state available to the agent. This delayed observation represents the state delay in the system. Furthermore, if there is an execution delay for the agent's actions, the action a_t decided at time t will only be executed at time $t+5$, meaning the action decided at time t is actually carried out at time $t+3$.

To address the aforementioned issue, we model the task offloading decision as a stochastic delay Markov decision process. This approach is employed to capture the randomness in the timing at which users observe the states and rewards associated with their tasks.

A. Stochastic Delay Markov Decision Process

In the realm of dynamic systems, the SDMDP represented by $\langle \mathcal{S}, \mathcal{A}, P_A, \mathcal{R}, O, AC, C, \gamma \rangle$ is crucial when some uncertainty in delays need to be dealt with, where O, AC, and C denote the random variables that represent the number of delay steps in observation, action, and cost, respectively [35]. It can also be simplified to a standard MDP represented by $\left\langle I_O, \mathcal{A}, P_A^O, r' \right\rangle$ [34]. The augmented state space I_O is $\mathcal{S} \times \mathcal{A}^{O+AC}$, incorporating the randomness in O and AC. It means the length of I_O is changing, reflecting the stochastic nature of delays. Furthermore, since delay is a random variable, agents might collect rewards repeatedly, because under partially observable conditions, agents may only partially observe system state at different time steps. Due to partial observability, it is crucial to include time information in the state space, leading to the redefinition of I_O as $\mathcal{S} \times \mathcal{A}^{O+AC} \times \mathbb{N}^+$. Specifically, the augmented state space at t is $I_t = \{s_{t-O}, t, a_{t-O}, a_{t-O+1}, \cdots, a_{t-1}\}$. If the action a_{t+1} is chosen, the state transitions to $I_{t+1} = \{s_{t-O+1}, t+1, a_{t-O+1}, a_{t-O+2}, \cdots, a_t\}$. Similar to DDMDP, the reward is defined as $r'(s_t, a_t) = \mathbb{E}[r(s_t, a_t)|I_t]$. Therefore, for an policy $\pi : \mathcal{S} \times \mathcal{A}^{O+AC} \times \mathbb{N}^+ \to \mathcal{A}$, considering the DDMDP$\langle \mathcal{S}, \mathcal{A}, P_A, r, O, AC = 0, C \rangle$ with observation-delay, the total expected reward is given by [36]

$$\begin{aligned} V_{obs}^{\pi}(I_t) &= \mathbb{E}_{\pi,O}\left[\sum_{l\geq t} \gamma^{(l-t)} r(s_{l-O}, a_{l-O})|I_t\right] \\ &= \mathbb{E}_{\pi,O}\left[\sum_{l\geq t-O} \gamma^{(l-t+O)} r(s_l, a_l)|I_t\right] \\ &= \mathbb{E}_{\pi,O}\left[\sum_{l\geq t-O} \gamma^{(l-t+O)} r(s_l, a_l)|I_t\right] \\ &+ \mathbb{E}_{\pi,O}\left[\sum_{l\geq t} \gamma^{(l-t+O)} r(s_l, a_l)|I_t\right], \end{aligned} \tag{28}$$

where $\gamma \in [0,1]$ is the discount factor. The goal is to maximize the total expected reward under observation delays, $V_{obs}^{\pi}(I_t)$, *i.e.*

$$\begin{aligned} &\arg\max_{\pi} V_{obs}^{\pi}(I_t) \\ &= \arg\max_{\pi} \mathbb{E}_{\pi,O}\left[\sum_{l\geq t} \gamma^{(l-t+O)} r(s_l, a_l)|I_t\right]. \end{aligned} \tag{29}$$

We consider DDMDP$\langle \mathcal{S}, \mathcal{A}, P_A, r, O = 0, AC, C \rangle$ with the action-delay. Then, the total expected reward is given by

$$\begin{aligned} V_{act}^{\pi}(I_t) &= \mathbb{E}_{\pi,AC}\left[\sum_{l\geq t} \gamma^{(l-t)} r(s_l, a_{l-AC})|I_t\right] \\ &= \mathbb{E}_{\pi,AC}\left[\sum_{l\geq t-AC} \gamma^{(l-t+AC)} r(s_{l+AC}, a_l)|I_t\right] \\ &= \mathbb{E}_{\pi,AC}\left[\sum_{l\geq t-AC} \gamma^{(l-t+AC)} r(s_{l+AC}, a_l)|I_t\right] \\ &+ \mathbb{E}_{\pi,AC}\left[\sum_{l\geq t} \gamma^{(l-t+AC)} r(s_{l+AC}, a_l)|I_t\right]. \end{aligned} \tag{30}$$

Similarly, for action delays, the objective is to maximize the total expected reward, $V_{act}^{\pi}(I_t)$, *i.e.*,

$$\begin{aligned} &\arg\max_{\pi} V_{act}^{\pi}(I_t) \\ &= \arg\max_{\pi} \mathbb{E}_{\pi,AC}\left[\sum_{l\geq t} \gamma^{(l-t+AC)} r(s_{l+AC}, a_l)|I_t\right]. \end{aligned} \tag{31}$$

VI. PROPOSED SOLUTION ALGORITHM

This section details our solution approach with DRL in LEO STINs with system state delay.

A. Design elements of DRL

When implementing DRL for LEO networks, we focus on three crucial components:

1) State and action variables: They include some critical variables for effective offloading decisions, such as user capacity, tasks, base station capacity, and connectivity.

2) Reward system: The reward system is designed to drive the learning process by minimizing the power consumption. It's structured as

$$r = \begin{cases} -E_s, & \text{if (22b)-(22j) are satisfied} \\ x, & \text{otherwise.} \end{cases} \tag{32}$$

where $x < 0$ is an empirical parameter and $-E_s$ is normalized during the agent training to ensure that it does not fall below x when the constraints are satisfied.

B. DRL for LEO STINs with Delay

We employ DDQN to train the task offloading agents which comprises of online network and target network with identical structures. The online network interacts directly with the system, tasked with collecting experiences and estimating action values, Q_{online}, while the target network is employed for the estimation of target values, Q_{target}. It is important to note that the parameters of target network are copied from the online network, and therefore, the target network does not engage in the learning process.

The learning process of DDQN is illustrated in Fig. 4, which incorporates an augmented experience pool to store the experience data collected during the system interactions

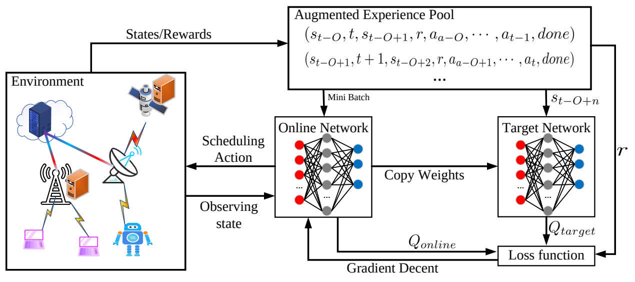

Fig. 4. The architecture of the DDQN scheme for task offloading.

and exhibits delay characteristics. The data, formatted as $(s_{t-O}, t, s_{t-O+1}, r, a_{a-O+1}, \cdots, a_t, done)$, provide learning material for training the online network. During the training phase, a mini-batch is randomly drawn from the augmented experience pool, enabling the online network to learn from historical experiences and optimize its decision-making strategy. The augmented experience pool is derived from the augmented state space described above.

Specifically, the action value, $Q_{online}(\theta^o, I_t, a_t, r)$, where $I_t = (s_{t-O}, t, a_{a-O}, \cdots, a_{t-1})$ is estimated through a neural network with parameter θ^o. The target value, $Q_{target}(\theta^g, I_{t+1}, a_t, r)$, with inputs $I_{t+1} = (s_{t-O+1}, t+1, a_{t-O+1}, \cdots, a_t)$, is similarly estimated by a neural network with the corresponding parameter θ^g. It is important to note that during the training process, θ^g is updated from θ^o after several iterations to ensure timely adjustments of the target network parameters. The loss function of DDQN aims to minimize the discrepancy between the outputs of the online and target networks. Thus, the loss function can been defined as

$$\begin{aligned}\mathcal{J}(\theta^o) &= \sum (Q_{target} - Q_{online})^2 + ||\theta^o||^2 \\ &= \sum (Q_{target}(I_{t+1}, \arg\max_a Q_{online}(I_t, a)) \\ &\quad + r - Q_{online}(I_t, a))^2 + ||\theta^o||^2,\end{aligned} \tag{33}$$

where $||\theta^o||^2$ represents the L_2 weight regularization, r denotes the reward calculated according to 32.

C. Complexity Analysis

The complexity of proposed algorithm mainly arises from two stages: DDQN agent training and DDQN deployment. We use two deep neural networks (DNN) as our core components where one DNN requires back propagation and the other one only performs inference. This is because DNN not only is simple to implement but also performs well in solving task offloading problems [43], as demonstrated in Section VII. So, the complexity of our DNN which requires back propagation is $O(N \cdot L \cdot M^2)$, where N is the number of training samples, L is the number of layers in the neural network, and M is the number of neurons per layer. For another, the complexity of our DNN which only performs inference is $O(L \cdot M^2)$. In summary, the total complexity for training stage is $O(N \cdot L \cdot M^2)$ while for deployment stage is $O(L \cdot M^2)$.

TABLE I
SYSTEM PARAMETERS

Parameter	Value	Parameter	Value
$f_{n,max}$	[5e7, 5×10^8]	$f_{m,max}$	[5e7, 5×10^8]
f_{max}^{cloud}	5e8	p_{bs}	1 J/s
f_k	[5e3, 10^4]	δ^2	7.9e-13 mW
α	2	ξ	1
p_l	30 J/s	p_{leo}	200 J/s
p_{cloud}	1000 J/s	p_k	40 J/s
p_k^{cloud}	100 J/s	p_k^{bs}	100 J/s

VII. PERFORMANCE EVALUATION

In this section, the simulation results are presented to illustrate the effectiveness of proposed task offloading algorithm in STINS.

A. Simulation Settings

The task offloading algorithm and neural network are implemented with Pytorch[1], LEO satellites are modeled using poliastro[2], and the system model is formulated by Python 3.7. We implement the proposed framework on a Linux workstation with 64-bit Ubuntu 22.04.1. The hardware for training all DRL baselines has one Nvidia's GPU with GeForce RTX 3090Ti with 24-GB memory. The CPU is an Intel(R) Core(TM) i9-10980XE processor, 18 cores, and 3.00GHz clock speed.

In the simulation, we consider a network scenario with a data center, 10 LEO satellites, 5 base stations, and 10 users. Each user has 1 task to process at each time slot and the input data size of computation tasks (in Mbit) is uniformly distributed in the range of $[10,000, 100,000]$. The output data size is uniformly distributed in the range of $[10, 100]$ and the corresponding number of required CPU cycles (in Megacycles) obeys uniform distribution in the range of $[10^4, 10^6]$. The transmission bandwidth allocation for the data center, low-Earth orbit satellites, and base stations are set to 100 MHz, 500 MHz, and 400 MHz, respectively. Other parameters are with reference to the setting of computing and communication in STINs [19], [40], [46], [47], the main parameters in our system are set as in Table I.

Additionally, we take a variety of baseline methods for comparisons, including DDQN [40], DQN [40], particle swarm optimization (PSO) [41], genetic algorithm (GA) [42], simulated annealing (SA), Random, and advantage actor-critic (A2C). We also compare four types of neural networks used in our proposed approach: convolutional neural network (CNN), DNN, gated neural network (GRU), and long short-term memory (LSTM) neural network. Among them, a two-layer convolutional neural network, two-layer feedforward fully connected neural network, one-layer gated neural network, and one-layer long short-term memory neural network are used and the learning rate for these neural networks is set to 0.001.

B. Performance Comparisons and Analysis

In the simulation experiments, we consider two scenarios: one is the system state delay and the other is the system action

[1]https://pytorch.org/
[2]https://github.com/poliastro/poliastro

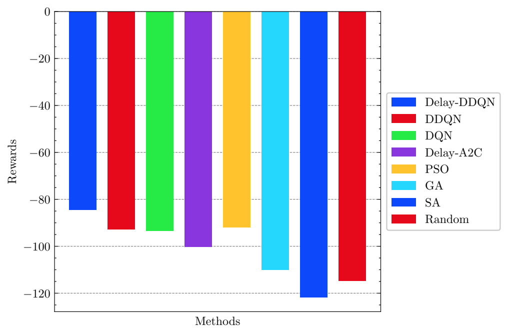

(a) Comparisons with stochastic system state delay.

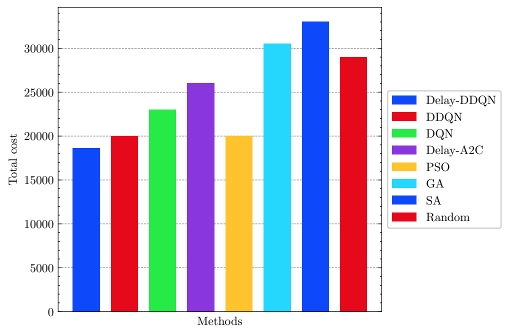

(b) Energy consumption comparisons with stochastic delay.

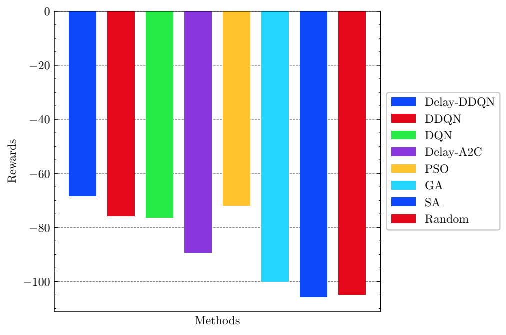

(c) Comparisons with action delays.

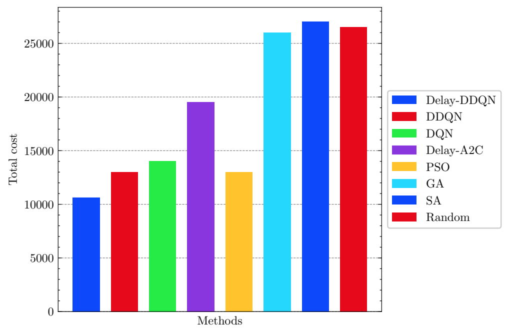

(d) Energy consumption comparisons with action delays.

Fig. 5. Main results.

delay. In addition, we also consider fixed system state and action delays as well as random system state and action delays.

1) Main Results: Fig. 5a shows the performance comparisons with random system state delays, where the Delay-DDQN outperforms other methods and reinforces its robustness and efficiency. Similarly, Fig. 5b presents the total energy consumption outcomes of various algorithms under the random system state delays. The Delay-DDQN method consistently outperforms the other evaluated methods, including traditional reinforcement learning approaches, such as DDQN and DQN, as well as heuristic-based methods, like PSO, GA, SA, and Random. This performance superiority highlights the effectiveness of the Delay-DDQN approach in handling tasks in dynamic and uncertain environments, further emphasizing its robustness and efficiency in stochastic settings.

In Fig. 5c and Fig. 5d which focus on the scenarios with action delays, the Delay-DDQN again demonstrates superior performance. Fig. 5c illustrates the reward outcomes of different methods in the presence of action delays and the Delay-DDQN achieves the higher rewards compared to other baselines. It indicates the capability to respond effectively despite the delays in executing actions. Fig. 5d shows the total energy consumption results for the same set of algorithms under the stochastic action delays. Here, the Delay-DDQN maintains lower costs than the other methods, underscoring its operational efficiency and advantage of incorporating delay-aware strategies in the optimization process. These results further validate the robustness and adaptability of the Delay-DDQN method, making it particularly suitable for the dynamic environments where the delays are inherent and unpredictable.

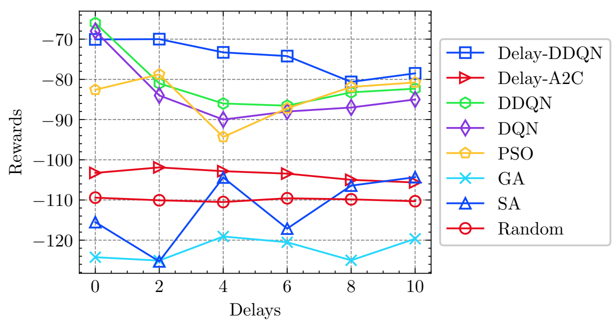

Fig. 6. Comparison of different algorithms under fixed state delays.

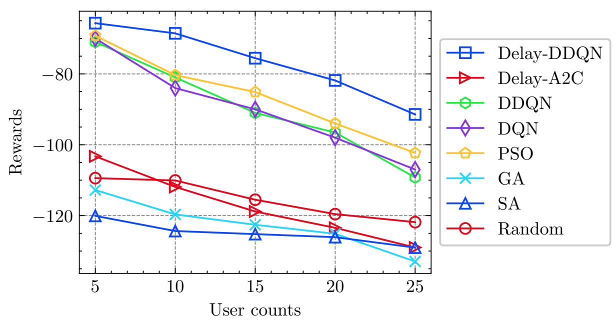

Fig. 7. Comparison of different algorithms when the number of users varies.

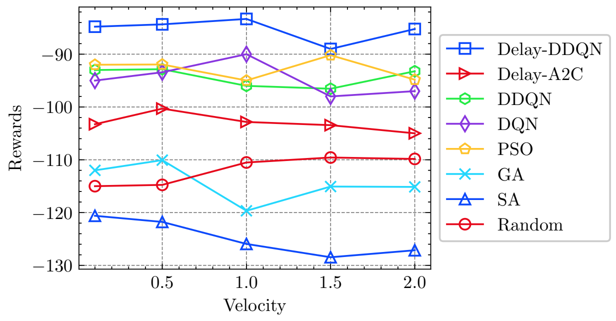

Fig. 8. Comparison of different algorithms when the velocity of users varies.

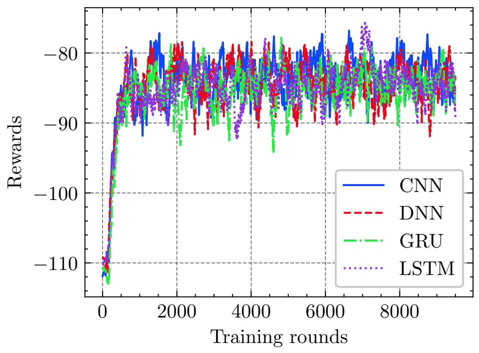

Fig. 9. Comparisons with neural networks for stochastic observation delays.

The results in Fig. 6 show that our proposed Delay-DDQN algorithm outperforms other benchmarks across various fixed state delay values, as evidenced by the consistently higher rewards it achieves. As the state delay increases, the performance of most algorithms declines, reflecting the challenge of making optimal decisions with delayed information. However, Delay-DDQN demonstrates remarkable resilience, maintaining relatively high rewards even at higher delay values, such as when the delay reaches 5 or more. This suggests that Delay-DDQN is particularly effective at handling delayed state information, likely due to its advanced processing of such delays within the decision-making framework. In comparison, other algorithms like Delay-A2C, DQN, and DDQN experience more significant drops in performance as delays increase, indicating their lower poorly in such scenarios. Traditional algorithms like PSO, GA, SA, and Random consistently perform robustness across all delay values, further underscoring the superiority of Delay-DDQN in environments with fixed state delays.

The results presented in Fig. 7 illustrate the performance of various algorithms as the number of users increases. The proposed Delay-DDQN algorithm consistently outperforms the other algorithms across all user counts, maintaining the highest rewards throughout. As the number of users increases, the rewards generally decrease for all algorithms, which is expected due to the increased competition for resources and the greater complexity in decision-making with more users. However, Delay-DDQN exhibits a more gradual decline in performance compared to other methods, indicating its superior capability in managing the increased load and complexity associated with a higher number of users. In contrast, algorithms such as Delay-A2C, PSO, DQN, and DDQN show decreases in rewards as the user count rises, reflecting their relatively lower effectiveness in handling scenarios with many users. Traditional optimization algorithms like GA, SA, and the Random strategy consistently perform the poorly across all user counts, further emphasizing the robustness of Delay-DDQN in user-dense environments.

The results in Fig. 8 show that the performance of various algorithms remains relatively stable as the user velocity changes, with our proposed Delay-DDQN algorithm consistently achieving the highest rewards across all velocity levels. Note that the values on the horizontal axis represent changes in speed. When the value is less than 1, the user's speed decreases, and when the value is greater than 1, the speed increases. This stability can be attributed to the architecture of STINs, which utilizes satellites with large coverage areas. Unlike ground-based networks, where user mobility can significantly affect communication and offloading decisions, the extensive coverage provided by satellites ensures that even at higher user velocities, the impact on task offloading and network performance is mild. As a result, Delay-DDQN maintains superior performance regardless of user speed, highlighting its effectiveness in dynamic environments. The results also indicate that while other algorithms like Delay-A2C, DQN, and DDQN show some variability, the overall influence of user velocity is limited due to the robust satellite coverage. Traditional optimization algorithms, such as PSO, GA, SA, and Random, perform consistently worse, but the effect of user velocity on their performance is less pronounced.

2) Ablation Studies on State Delays: Fig. 9 shows the experimental results under the conditions with random system state delays which varies from 0 to 10. It can been seen that regardless of the type of used neural network, the rewards fluctuate within a certain range. This indicates that the proposed method is effective in situations where the system state delay is random. Furthermore, the experimental results in Fig. 9 suggest that in cases of random system state delays, it is advisable to choose neural networks that have faster training efficiency and inference speed. Moreover, Fig. 9 also shows that the neural networks are unstable during the training. Despite careful tuning during the experiments, the issue of training instability could not be alleviated, which may be due to the more severe system dynamic changes caused by the random system state delays.

Fig. 10 depicts the loss value trends of various neural networks in DDQN under the conditions of random system state delays. The results indicate that during the early stage of training, the loss value quickly rises from 2.25 to around 4.4, then continuously decreases, and finally oscillates within a certain range. In the initial phase of training, due to the presence of system state delays and the inability to collect system feedback, including the system rewards, the loss value rapidly increases to around 4.4. Afterwards, the loss value begins to decrease and oscillates within a range, which shows that the proposed method has a certain learning capability. This oscillation of loss values briefly leads to a time-variant optimization performance in each neural network. About the

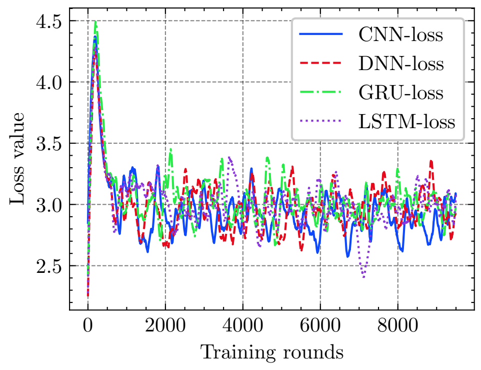

Fig. 10. Comparisons with neural networks for loss value.

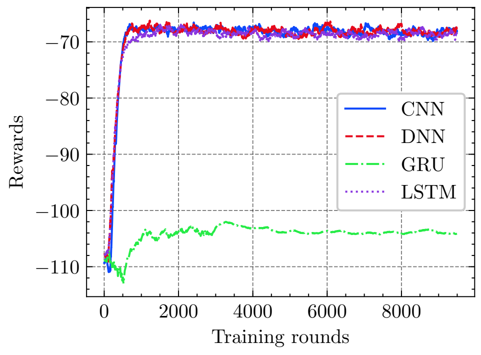

Fig. 11. Comparisons with neural networks for stochastic action delays.

above simulation results, the neural network performs differently under both fixed system state delay and random system state delay. Overall, the results validate the effectiveness of proposed method.

3) Ablation Studies on Action Delays: Fig. 11 presents the experimental results under the conditions with random system action delays which varies from 0 to 10. The results show that except for the GRU neural network, the rewards for CNN, DNN, and LSTM neural networks fluctuate within a certain range. It can be observed that the type of neural network affects the performance of proposed method and the loss value of the GRU neural network does not converge, leading to poorer performance, as shown in Fig. 12. Similarly, in the early stages of training, the loss value quickly rises from 2.2 to around 4.3, then continuously decreases, and finally oscillates within a certain range. The rapid increase in loss value in the early stages is due to the presence of system state delays and the inability to collect system feedback, including system rewards. The subsequent decrease and oscillation in loss value indicate that the proposed method has a certain learning capability. This figure demonstrates that whether the loss value converges during the training period of proposed method does not affect our task offloading performance. Therefore, considering the training stability of proposed method is important when there are system action delays.

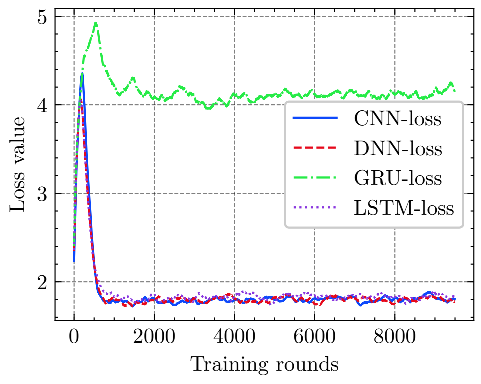

Fig. 12. Comparisons with neural networks for loss value on stochastic action delays.

4) Analysis of Computing Resource Allocation: Fig. 13 demonstrates the performance improvement of RAMLFQ over the traditional Multi-Level Feedback Queue (MLFQ) through two metrics: average turnaround time and average waiting time. Fig. 13a illustrates the impact of task number on the average turnaround time. Compared with MLFQ, RAMLFQ exhibits significantly lower turnaround times across all task quantity configurations which indicates its more efficient management of task execution. Particularly, as the number of tasks increases, the performance advantage of RAMLFQ becomes more evident which shows its effective resource management under the high load conditions. Fig. 13b provides a view of the effect of task number on the average waiting time. RAMLFQ offers a lower waiting time in most scenarios, especially when the task number is high. It underscores the ability of RAMLFQ to reduce the waiting times when handling a large volume of tasks. This is because of its fine-grained management in terms of priorities and resource constraints. Furthermore, Fig. 13c displays a comparison of the average response time between RAMLFQ and MLFQ algorithms under different task numbers. In most cases, the response time of RAMLFQ is higher than that of MLFQ. This increase in response time in RAMLFQ is because of the adoption of more fine-grained priority and the dynamic allocation strategy in allocating computing resources. It means that RAMLFQ tends to give preference to high-priority or resource-intensive tasks during the resource allocation, and these tasks require a longer time to respond. Moreover, the longer response time might also reflect RAMLFQ's efforts to ensure fairness in resource allocation, which might lead to a slight delay in responding to certain tasks so that the system can serve all tasks more equitably. Although RAMLFQ's response time is marginally higher than MLFQ, its advantages in terms of turnaround time and waiting time might more effectively demonstrate its superior performance in dynamic and complex computing environments. This suggests that the RAMLFQ strategy has significant advantages in terms of adaptability and flexibility in meeting diverse task requirements.

VIII. CONCLUSION

Due to network entity mobility, architecture variation, and user heterogeneity, STINs often experience various system state delays which will bring out significant challenges for computation offloading and resource allocation issues. In this

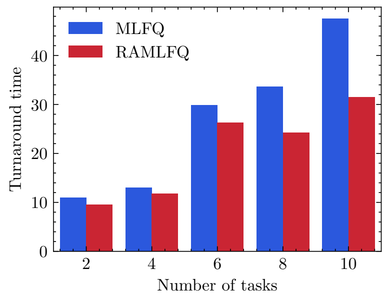

(a) Average turnaround time by task number

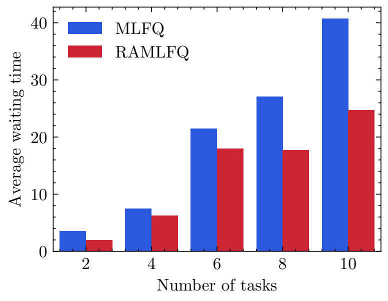

(b) Average waiting time by task number

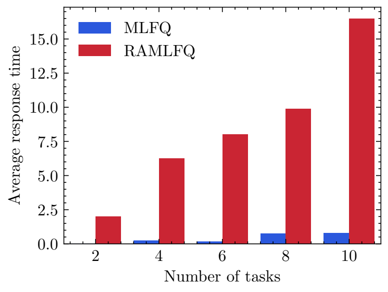

(c) Average respons time by task number

Fig. 13. The performance of computing resource allocation based on CPU task scheduling.

paper, we have jointly considered the computation offloading and resource allocation to address the system state delay problem. We have explored the computation offloading challenge in LEO STINs, particularly focusing on the system state delay. We also have proposed a multi-level feedback queue for computing allocation and a state augmentation DRL task scheduling mechanism. These solutions efficiently allocate the computing resources across various edge servers, including base stations and LEO satellites. To mitigate the impact of system state delay, we have employed stochastic delay MDPs to formulate the problem and then formulated a state-augmented DRL-based computation offloading approach to seek an optimal offloading mode. The utilization of deep neural networks and DDQN significantly enhanced the learning performance. Finally, the simulation results have confirmed the effectiveness of the proposed approaches.

In the future, we will explore the use of digital twins in STINs to accurately model real-world scenarios, ensuring smoother transitions from simulation to deployment. This approach is crucial for enhancing the reliability and performance of deep reinforcement learning models in practical applications. Moreover, we will also consider the use of phased array antennas in LEO satellites and base stations, as well as account for interbeam interference and interference between cellular and satellite coverage.

REFERENCES

[1] T. Pfandzelter and D. Bermbach, “Edge (of the earth) Replication: Optimizing Content Delivery in Large LEO Satellite Communication Networks,” in *Proc. IEEE/ACM CCGrid*, Melbourne, VIC, Australia, May. 2021, pp. 565¨C575.

[2] C. Ding, J. -B. Wang, M. Cheng, M. Lin and J. Cheng, “Dynamic Transmission and Computation Resource Optimization for Dense LEO Satellite Assisted Mobile-Edge Computing,” *IEEE Trans. Commun.*, vol. 71, no. 5, pp. 3087-3102, May. 2023.

[3] D. Wang, T. He, Y. Lou, L. Pang, Y. He and H. -H. Chen, “Double-edge Computation Offloading for Secure Integrated Space-air-aqua Networks”, *IEEE Internet Things J.*, vol. 10, no. 17, pp. 15581-15593, Sep. 2023.

[4] Q. Tang, Z. Fei, B. Li and Z. Han, “Computation Offloading in LEO Satellite Networks With Hybrid Cloud and Edge Computing,” *IEEE Internet Things J.*, vol. 8, no. 11, pp. 9164-9176, Jun. 2021.

[5] Q. Tang, Z. Fei, B. Li, H. Yu, Q. Cui, J. Zhang and Z. Han, “Stochastic Computation Offloading for LEO Satellite Edge Computing Networks: A Learning-Based Approach,” *IEEE Internet Things J.*, pp. 1-1, Aug. 2023.

[6] H. Zhang, S. Xi, H. Jiang, Q. Shen, B. Shang and J. Wang, “Resource Allocation and Offloading Strategy for UAV-Assisted LEO Satellite Edge Computing”. *Drones*, vol. 7, no. 6, pp. 383, 2023.

[7] Z. Ji, S. Wu and C. Jiang, “Cooperative Multi-Agent Deep Reinforcement Learning for Computation Offloading in Digital Twin Satellite Edge Networks,” *IEEE J. Sel. Areas Commun.*, vol. 41, no. 11, pp. 3414-3429, Nov. 2023.

[8] S. Fujimoto, H. Hoof and D. Meger. “Addressing Function Approximation Error in Actor-critic Methods”. in *Proc. Int. conf. mach. learn.*, 2018, pp. 1587-1596.

[9] S. Sthapit, S. Lakshminarayana, L. He, G. Epiphaniou and C. Maple, “Reinforcement Learning for Security-Aware Computation Offloading in Satellite Networks,” *IEEE Internet Things J.*, vol. 9, no. 14, pp. 12351-12363, Jul, 2022.

[10] G. Cui, Y. Long, L. Xu and W. Wang, “Joint Offloading and Resource Allocation for Satellite Assisted Vehicle-to-Vehicle Communication,” *IEEE Syst. J.*, vol. 15, no. 3, pp. 3958-3969, Sep. 2021.

[11] S. Nath, M. Baranwal and H. Khadilkar, “Revisiting state augmentation methods for reinforcement learning with stochastic delays”, in *Proc. ACM. Int. Conf. Inf. Knowl. Manage.*, 2021, pp. 1346-1355.

[12] R. Xie, Q. Tang, Q. Wang, X. Liu, F. R. Yu and T. Huang, “Satellite-Terrestrial Integrated Edge Computing Networks: Architecture, Challenges, and Open Issues,” *IEEE Network*, vol. 34, no. 3, pp. 224-231, May./Jun. 2020.

[13] Q. Zhang, Y. Luo, H. Jiang and K. Zhang, “Aerial Edge Computing: A Survey,” *IEEE Internet Things J.*, vol. 10, no. 16, pp. 14357-14374, 15 Aug. 2023.

[14] Y. Lin, W. Feng, T. Zhou, Y. Wang, Y. Chen, N. Ge and C. Wang, “Integrating Satellites and Mobile Edge Computing for 6G Wide-Area Edge Intelligence: Minimal Structures and Systematic Thinking,” *IEEE Network*, vol. 37, no. 2, pp. 14-21, Mar./Apr. 2023.

[15] Z. Zhang, W. Zhang and F. -H. Tseng, “Satellite Mobile Edge Computing: Improving QoS of High-Speed Satellite-Terrestrial Networks Using Edge Computing Techniques,” *IEEE Network*, vol. 33, no. 1, pp. 70-76, Jan./Feb. 2019.

[16] Z. Lin, M. Lin, T. de Cola, J. -B. Wang, W. -P. Zhu and J. Cheng, “Supporting IoT With Rate-Splitting Multiple Access in Satellite and Aerial-Integrated Networks,” *IEEE Internet Things J.,* vol. 8, no. 14, pp. 11123-11134, 15 July15, 2021.

[17] G. Valecce, S. Strazzella, and L. A. Grieco, “On the interplay between 5G, mobile edge computing and robotics in smart agriculture scenarios,” *Proc. 18th Int. Conf. Ad-Hoc Netw. Wireless (ADHOC-NOW 2019),* Luxembourg, Luxembourg, Oct. 1-3, 2019, pp. 549-559.

[18] J. Du, C. Jiang, A. Benslimane, S. Guo and Y. Ren, “SDN-Based Resource Allocation in Edge and Cloud Computing Systems: An Evolutionary Stackelberg Differential Game Approach,” *IEEE/ACM Trans. Networking*, vol. 30, no. 4, pp. 1613-1628, Aug. 2022.

[19] X. Cao et al., “Edge-Assisted Multi-Layer Offloading Optimization of LEO Satellite-Terrestrial Integrated Networks,” *IEEE J. Sel. Areas Commun.*, vol. 41, no. 2, pp. 381-398, Feb. 2023.

[20] Z. Lin, M. Lin, B. Champagne, W. -P. Zhu and N. Al-Dhahir, “Secrecy-Energy Efficient Hybrid Beamforming for Satellite-Terrestrial Integrated Networks,” *IEEE Trans. Commun.,* vol. 69, no. 9, pp. 6345-6360, Sept. 2021.

[21] J. von Mankowski, E. Durmaz, A. Papa, H. Vijayaraghavan and W. Kellerer, “Aerial-Aided Multiaccess Edge Computing: Dynamic and Joint Optimization of Task and Service Placement and Routing in Multilayer Networks,”*IEEE Trans. Aerosp. Electron. Syst.*, vol. 59, no. 3, pp. 2593-2607, Jun. 2023.

[22] X. Zhang, J. Liu, R. Zhang, Y. Huang, J. Tong, N. Xin, L. Liu and Z.

Xiong, "Energy-Efficient Computation Peer Offloading in Satellite Edge Computing Networks," *IEEE Trans. Mob. Comput.*, pp. 1-15, Apr. 2023.

[23] Q. Li, S. Wang, X. Ma, Q. Sun, H. Wang, S. Cao and F. Yang, "Service Coverage for Satellite Edge Computing," *IEEE Internet Things J.*, vol. 9, no. 1, pp. 695-705, Jan. 2022.

[24] C. Ding, J. -B. Wang, H. Zhang, M. Lin and G. Y. Li, "Joint Optimization of Transmission and Computation Resources for Satellite and High Altitude Platform Assisted Edge Computing," *IEEE Trans. Wireless Commun.*, vol. 21, no. 2, pp. 1362-1377, Feb. 2022.

[25] J. Liu, X. Zhao, P. Qin, S. Geng and S. Meng, "Joint Dynamic Task Offloading and Resource Scheduling for WPT Enabled Space-Air-Ground Power Internet of Things," *IEEE Trans. Network Sci. Eng.*, vol. 9, no. 2, pp. 660-677, Mar./Apr. 2022.

[26] Y. Yin, C. Huang, D. Wu and S. Huang, "Joint Computation Offloading and Resource Allocation in Space-air-terrestrial Integrated Networks for IoT Applications". *Ad Hoc Networks*, vol. 150, pp. 103267, Aug. 2023.

[27] Y. Liu, L. Jiang, Q. Qi, K. Xie and S. Xie, "Online Computation Offloading for Collaborative Space/Aerial-Aided Edge Computing Toward 6G System". *IEEE Trans. Veh. Technol.*, pp. 1-11, Sep. 2023.

[28] B. Mao, F. Tang, Y. Kawamoto and N. Kato, "Optimizing Computation Offloading in Satellite-UAV-Served 6G IoT: A Deep Learning Approach," *IEEE Network*, vol. 35, no. 4, pp. 102-108, Jul./Aug. 2021.

[29] S. Yu, X. Gong, Q. Shi, X. Wang and X. Chen, "EC-SAGINs: Edge-Computing-Enhanced Space¨CAir¨CGround-Integrated Networks for Internet of Vehicles," *IEEE Internet Things J.*, vol. 9, no. 8, pp. 5742-5754, Apr. 2022.

[30] G. Cui, P. Duan, L. Xu and W. Wang, "Latency Optimization for Hybrid GEO¨CLEO Satellite-Assisted IoT Networks," *IEEE Internet Things J.*, vol. 10, no. 7, pp. 6286-6297, Apr. 2023.

[31] H. Zhang, R. Liu, A. Kaushik and X. Gao, "Satellite Edge Computing With Collaborative Computation Offloading: An Intelligent Deep Deterministic Policy Gradient Approach," *IEEE Internet Things J.*, vol. 10, no. 10, pp. 9092-9107, May, 2023.

[32] N. Waqar, S. A. Hassan, A. Mahmood, K. Dev, D. -T. Do and M. Gidlund, "Computation Offloading and Resource Allocation in MEC-Enabled Integrated Aerial-Terrestrial Vehicular Networks: A Reinforcement Learning Approach," *IEEE Trans. Intell. Transp. Syst.*, vol. 23, no. 11, pp. 21478-21491, Nov. 2022.

[33] S. S. Hassan, Y. M. Park, Y. K. Tun, W. Saad, Z. Han and C. S. Hong, "Satellite-Based ITS Data Offloading & Computation in 6G Networks: A Cooperative Multi-Agent Proximal Policy Optimization DRL With Attention Approach," *IEEE Trans. Mob. Comput.*, pp. 1-18, Aug. 2023.

[34] E. Altman and P. Nain, "Closed-loop Control with Delayed Information," *Perf. Eval. Rev.*, vol. 14, pp. 193-204, 1992.

[35] K. V. Katsikopoulos and S. E. Engelbrecht, "Markov Decision Processes with Delays and Asynchronous Cost Collection," *IEEE Trans. Autom. Control.*, vol. 48, no. 4, pp. 568-574, Apr. 2003.

[36] C. J. C. H. Watkins and P. Dayan, "Q-learning," *Mach. Learn.*, vol. 8, pp. 279-292, 1992.

[37] F. J. Corbat¨®, M. Merwin-Daggett and R.C. Daley, "An experimental time-sharing system", in *Proc. Spring. Joint. Comput. Conf.*, 1962, pp. 335-344.

[38] A. U. Chaudhry and H. Yanikomeroglu, "Laser Intersatellite Links in a Starlink Constellation: A Classification and Analysis," *IEEE Veh. Technol. Mag.*, vol. 16, no. 2, pp. 48-56, Jun. 2021.

[39] Z. Lin, H. Niu, K. An, Y. Wang, G. Zheng, S. Chatzinotas, and Y. Hu, "Refracting RIS-Aided Hybrid Satellite-Terrestrial Relay Networks: Joint Beamforming Design and Optimization," *IEEE Trans. Aerosp. Electron. Syst.,* vol. 58, no. 4, pp. 3717-3724, Aug. 2022.

[40] N. Cheng, F. Lyu, W. Quan, C. Zhou, H. He, W. Shi and X. Shen, "Space/Aerial-Assisted Computing Offloading for IoT Applications: A Learning-Based Approach," *IEEE J. Sel. Areas Commun.*, vol. 37, no. 5, pp. 1117-1129, May. 2019.

[41] X. Gao, H. Yingmeng, S. Yingzhao, Z. Hangyu, L. Yang, L. Rongke and Z. Jianhua, "Hierarchical Dynamic Resource Allocation for Computation Offloading in LEO Satellite Networks," *IEEE Internet Things J.*, vol. 11, no. 11, pp. 19470-19484, Jun. 2024.

[42] G. Cui, P. Duan, L. Xu and W. Wang, "Latency Optimization for Hybrid GEO-LEO Satellite-Assisted IoT Networks," *IEEE Internet Things J.*, vol. 10, no. 7, pp. 6286-6297, Apr. 2023.

[43] H. Zhai, X. Zhou, H. Zhang and D. Yuan, "Delay Minimization in Hybrid Edge Computing Networks: A DDQN-Based Task Offloading Approach," *IEEE Trans. Veh. Technol.*, pp. 1-11, May. 2024.

[44] P. Wei, W. Feng, Y. Wang, Y. Chen, N. Ge and C. -X. Wang, "Joint Mobility Control and MEC Offloading for Hybrid Satellite-Terrestrial-Network-Enabled Robots," *IEEE Trans. Wireless Commun.*, vol. 22, no. 11, pp. 8483-8497, Nov. 2023.

[45] Z. Lin, M. Lin, J. -B. Wang, T. de Cola and J. Wang, "Joint Beamforming and Power Allocation for Satellite-Terrestrial Integrated Networks With Non-Orthogonal Multiple Access," *IEEE J. Sel. Top. Signal Process.,* vol. 13, no. 3, pp. 657-670, June 2019.

[46] Y. Wang and K.A. Gui, "Optimization of Energy Use in Radio Frequency Transmission for Satellite Communication," *Computer Communications*, vol. 211, pp. 73-82, Nov. 2023.

[47] J. Lorincz, T. Garma and G. Petrovic, "Measurements and Modelling of Base Station Power Consumption under Real Traffic Loads", *Sensors*, vol. 12, no. 4, pp. 4281-4310, Mar. 2012.